*Research Article*

# Enhancement of Photocatalytic Activity on TiO$_2$-Nitrogen-Doped Carbon Nanotubes Nanocomposites

## Lingling Wang,[1] Long Shen,[2] Yihuai Li,[1] Luping Zhu,[1] Jiaowen Shen,[1] and Lijun Wang[1]

[1] *School of Urban Development and Environment Engineering, Shanghai Second Polytechnic University,*
 *2360 Jinhai Road, Shanghai 201209, China*
[2] *Shanghai Shanshan Technology Co., Ltd., 3158 Jinhai Road, Shanghai 201209, China*

Correspondence should be addressed to Lijun Wang; wang_lijun@yahoo.cn

TiO$_2$-nitrogen-doped carbon nanotubes (TiO$_2$-CNx) nanocomposites are successfully synthesized via a facile hydrothermal method. The prepared photocatalysts were systematically characterized by X-ray diffraction (XRD), scanning electron microscopy (SEM), transmission electron microscopy (TEM), and thermogravimetric and differential scanning calorimetry analyses (TGA-DSC). The results show that the TiO$_2$ nanoparticles with a narrow size of 7 nm are uniformly deposited on CNx. The photocatalytic activity of the nanocomposite was studied using methyl orange (MO) as a model organic pollutant. The experimental results revealed that the strong linkage between the CNx and TiO$_2$ played a significant role in improving photocatalytic activity. However, the mechanical process for CNx and TiO$_2$ mixtures showed lower activity than neat TiO$_2$. Moreover, TiO$_2$-CNx nanocomposites exhibit much higher photocatalytic activity than that of neat TiO$_2$ and TiO$_2$-CNTs nanocomposites. The improved photodegradation performances are attributed to the suppressed recombination of electrons and holes caused by the effective transfer of photogenerated electrons from TiO$_2$ to CNx.

## 1. Introduction

Photocatalysis has been widely applied as a technique of destruction of organic pollutants due to its high performance, low cost, nontoxicity, stability, and availability [1, 2]. Titanium dioxide (TiO$_2$), a semiconductor with direct bandgap of 3.2 eV, has excellent photocatalytic properties and chemical stability, and it is an environmentally friendly and abundant substance [3, 4]. However, a major limitation to achieve high photocatalytic efficiency is the quick recombination of photo-generated charge carries [5]. Recombination has faster kinetics than surface redox reactions and greatly reduces the quantum efficiency of photocatalysis. Therefore, currently a particularly attractive option is to design and develop hybrid materials based on TiO$_2$ to solve this problem.

Recently, carbon-based nanomaterials, such as carbon nanotubes (CNTs) and graphene, have been reported as the hybrid component to be incorporated into TiO$_2$ due to their unique electrical properties, superior chemical stability, and good conductivity. The common approaches to synthesize TiO$_2$-CNTs composites include sol-gel method [6, 7], chemical vapor deposition (CVD) [8, 9], and electrospinning [10]. Various structural forms of titania-carbon nanotubes photocatalysts have been prepared, such as TiO$_2$ nanoparticles on CNTs [11], TiO$_2$ layer coating on aligned CNTs arrays [12], CNTs incorporating into the TiO$_2$ film [13], TiO$_2$ layer coating on CNTs [14], and low loading amounts of CNTs embedded inside mesoporous TiO$_2$ aggregates [15]. Cong et al. [16] have prepared uniform and fine well-dispersed carbon-doped TiO$_2$ coating on multiwalled carbon nanotubes by oxidation of titanium-carbide-(TiC-) coated CNTs, and the prepared carbon-doped TiO$_2$ coating on CNTs shows a higher visible light photocatalytic activity.

However, to fabricate the TiO$_2$-CNTs composites, the CNTs required a pretreatment process to modify their inert surface nature via harsh processes for activation by refluxing in concentrated acids, which destroys the $\pi$ conjugation and reduces the conductance of the CNTs base [17]. Unfavorably,

the harsh process would risk CNTs to some damages in their inherent properties. To bypass the drawbacks suffered by CNTs, employing CNx without requiring any pretreatment to composite with the functional materials directly is a promising method because the nitrogen atoms on the surface of the CNTs modify the adsorption strength of the nanotubes towards foreign elements. Moreover, nitrogen atoms in the framework of CNx will form chemically active points which are available for metal or metallic oxide nanoparticles anchoring. Ghosh and coworkers [17] prepared ZnO/CNx composites via a simple wet-chemical method and studied their field emission performance. CNx decorated with $CeO_2$ and $SnO_2$ nanoparticles showed greater activity and sensitivity than the conventional CNT-based composites for NO electrooxidation [18].

In this work, according to the unique properties of CNx, we have synthesized $TiO_2$-CNx nanocomposites with different weight ratios via a facile hydrothermal method. The resulting materials were well characterized for their physicochemical properties, structural features, as well as potential applications to the photodegradation of MO.

## 2. Experimental

*2.1. Synthesis of $TiO_2$-CNx.* Following the procedures reported previously [19], CNx was synthesized using diethylamine as the carbon and nitrogen source. The purification process for CNx was as follows: CNx was firstly washed three times by 20% HF solution, then soaked in 20% HF solution overnight, gathered by filtration, and finally dried at 80°C for 2 h.

$TiO_2$-CNx nanocomposites were prepared using a hydrothermal synthesis method. CNx was added to provide a weight ratio of $TiO_2$ over CNx in the range from 5% to 20%, indicated with X wt% $TiO_2$-CNx. CNx was initially dispersed into a 30 mL solution containing 2.7 mL water and 27.3 mL isopropanol, and the suspension was treated by sonication overnight. Then the titanium precursor solution, 3.41 mL titanium isopropoxide in 18 mL isopropanol was added dropwise into the CNx suspension under vigorous stirring. The mixture was left at room temperature under stirring for 2 h to complete the hydrolysis reaction. The mixed solution was then transferred into a teflon-lined stainless-steel autoclave (50 mL capacity). The autoclave was maintained at 140°C for 24 h and then cooled down to room temperature. The resulting solid was washed with ethanol and deionized water, gathered by filtration, and subsequently dried at 80°C overnight. The $TiO_2$-CNx solids were ground into powder and stored in a dessicator for further usage. For comparison, $TiO_2$-CNTs composites were synthesized using the similar procedures besides CNTs pretreated in concentrated $HNO_3$ at 140°C for 14 h, and neat $TiO_2$ sample was synthesized without adding CNTs.

*2.2. Characterization.* The bare CNx and the composites were characterized by a wide range of analytical techniques. The degree of crystallinity of the $TiO_2$-CNx composites was characterized by powder X-ray diffraction (XRD). The XRD patterns with diffraction intensity versus $2\theta$ were recorded
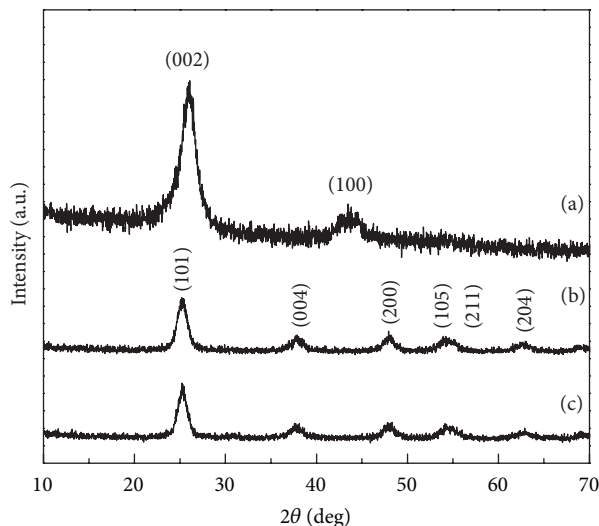


FIGURE 1: XRD patterns of bare CNx (a) and $TiO_2$-CNx composites with different weight ratio of $TiO_2$ over CNx 5% (b) and 20% (c).

in a Bruker D8 ADVANCE instrument with Cu-Kα radiation ($\lambda = 1.5418$ Å) from 20° to 70° at a scanning speed of 2°/min. X-ray tube voltage and current were set at 40 kV and 40 mA, respectively. Thermogravimetric and differential scanning calorimetry analyses (TGA-DSC) were performed by a Netzsch STA-449C analyzer with a heating rate of 10°C/min and an air flow rate of 100 mL/min. Scanning electron microscopy (SEM) was carried out on Hitachi S-4800 with an acceleration voltage of 5 kV. Transmission electron microscopy (TEM) was carried out on JEOL-JEM-1005 at 200 kV. The specimens for SEM and TEM imaging were prepared by suspending solid samples in ethanol with 15 min ultrasonication and placing a drop of this mixture on a 3.05 mm diameter copper mesh, which was then dried in air.

*2.3. Photodegradation of MO.* The photoreactor was designed with a cylindrical quartz cell configuration and an internal light source surrounded by a quartz jacket, where MO aqueous solution completely surrounded the light source. An external cycled cooling flow of water was used to maintain the reaction temperature constant.

Photocatalytic experiments were carried out by adding 0.01 g $TiO_2$ or $TiO_2$-CNTs composites or $TiO_2$-CNx composites into photoreactor containing 30 mL MO solution with an initial concentration of 15 mg/L. The mixture was stirred for 30 min in the dark to favor the adsorption equilibration, and then the stirred suspensions were illuminated with a 300 W high-pressure mercury lamp 10 cm high over the solution. The solution was stirred continuously during the photocatalytic reaction. The concentration of MO was analyzed by recording the absorption band maximum at 464 nm in the absorption spectra, using Shimadzu UV-2550 spectrophotometer.

## 3. Results and Discussion

The XRD patterns of the bare CNx and $TiO_2$-CNx nanocomposites are shown in Figure 1. The main peaks at 26.1° and
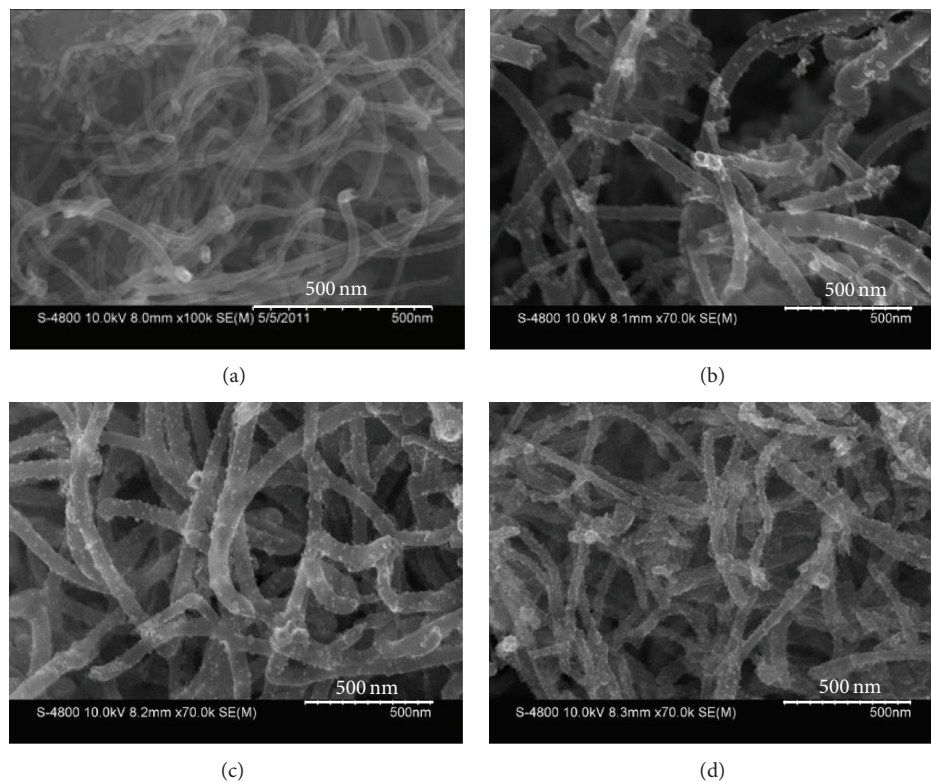
FIGURE 2: SEM images of bare CNx (a), TiO$_2$-CNx composites with different weight ratio of TiO$_2$ over CNx 5% (b), 10% (c), and 20% (d).

42.6° corresponded to the (002) and (100) reflections of CNx, respectively, (JCPDS 41-1487), which indicated that the employed CNx was highly graphitized (Figure 1(a)). It is obvious that the TiO$_2$-CNx nanocomposites show the same characteristic diffraction peaks referred to as anatase TiO$_2$ (JCPDS number 21-1272). The characteristic peaks at $2\theta$ of 25.3, 37.8, 48.0, 53.9, 55.1, and 62.7° can be indexed to (101), (004), (200), (105), (211), and (204) crystal planes of anatase TiO$_2$, respectively. Notably, no typical diffraction peaks belonging to the separate CNx are observed in the TiO$_2$-CNx nanocomposites. The reason can be ascribed to the fact that the main characteristic peak of CNx at 26.1° might be shielded by the main peak of anatase TiO$_2$ at 25.3°.

Figures 2 and 3 show the SEM and TEM images of bare CNx and TiO$_2$-CNx composites. CNx with relatively outer diameter (30~60 nm) was obtained, and the nanomaterial has a bamboo-like morphology with a clear, smooth surface. It is clearly seen that, for TiO$_2$-CNx nanocomposites, the TiO$_2$ nanoparticles are almost uniformly deposited on the surface of CNx. The more weight ratio of TiO$_2$ over CNx, the more visible nanoparticles observed (Figures 2(b), 2(c), and 2(d)). Figure 3(b) is TEM image of an individual CNx fully coated with TiO$_2$ nanoparticles. The bamboo-like morphology of CNx can be also clearly observed, and its surface is entirely and homogeneously covered by TiO$_2$ nanoparticles. There are no clear boundary and vacant space between the TiO$_2$ coating and CNx substrate. The nanoparticles covered on the CNx show clear crystal lattice fringes (Figure 3(c)). The intimate contact between CNx and TiO$_2$ favors the formation of junctions between the two materials, as a result, being helpful for improving the charge separation and thus the photocatalytic activity. As estimated from the TEM images, the size of TiO$_2$ nanoparticles is about 7 nm. EDX spectrum presented in Figure 3(d) further determined the existence of Ti and O atoms.

TGA-DSC analysis was carried out to estimate the carbon nanotube content of the nanocomposite. The results of weight loss and heat flow as a function of temperature for TiO$_2$-CNx nanocomposites are shown in Figure 4. For the 5 wt% and 15 wt% TiO$_2$-CNx nanocomposites, the weight loss due to the combustion of the CNx was 93.5% and 83.8%, respectively, indicating that TiO$_2$/CNx ratios estimated from the synthesis precursors of the nanocomposites were in close agreement with the results obtained from TGA-DSC analyses. Therefore, negligible losses of CNx occurred during the composite preparation procedure. The combustion point of CNx in the 15 wt% TiO$_2$-CNx composite was found to be 544.3°C, whereas CNx in 5 wt% TiO$_2$-CNx composite could not be combusted until approximately 647.6°C. The combustion temperature shift between different TiO$_2$/CNx ratios may be ascribed to the following two reasons: (i) more amount of TiO$_2$ grafted on the sidewall of CNx may provide more oxygen required by the combustion of CNx and (ii) more amount of TiO$_2$ restrains the heat transfer creating localized hot spots, facilitating the oxidation of carbon.

Figure 5 shows the results of the decomposition of MO under irradiation, in the presence of neat TiO$_2$, TiO$_2$-CNTs, and TiO$_2$-CNx nanocomposites with different weight
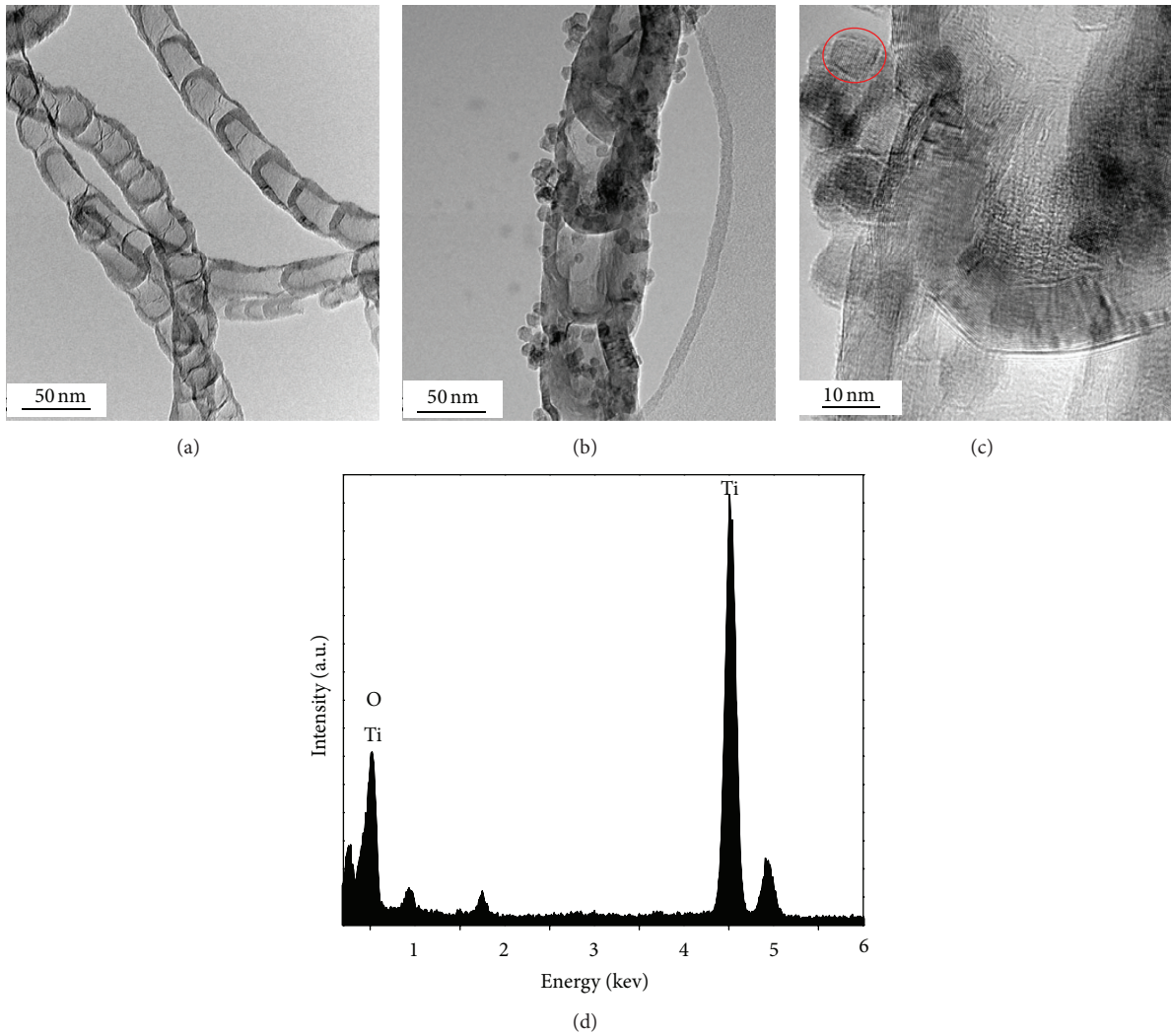
(a)



(b)



(c)



(d)

FIGURE 3: TEM images of bare CNx (a), low-magnification TEM image (b), high-magnification TEM image (c), and EDS spectrum of 10 wt% $TiO_2$-CNx composites (d).
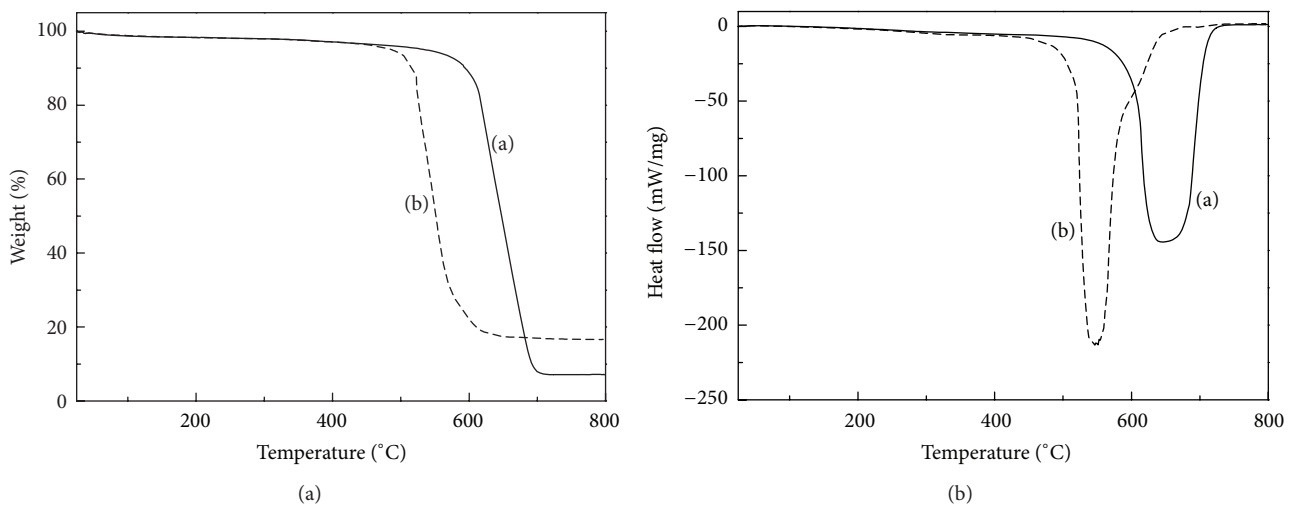


(a)



(b)

FIGURE 4: TG and DSC curves of $TiO_2$-CNx composites with different weight ratio of $TiO_2$ over CNx 5% (a) and 15% (b).
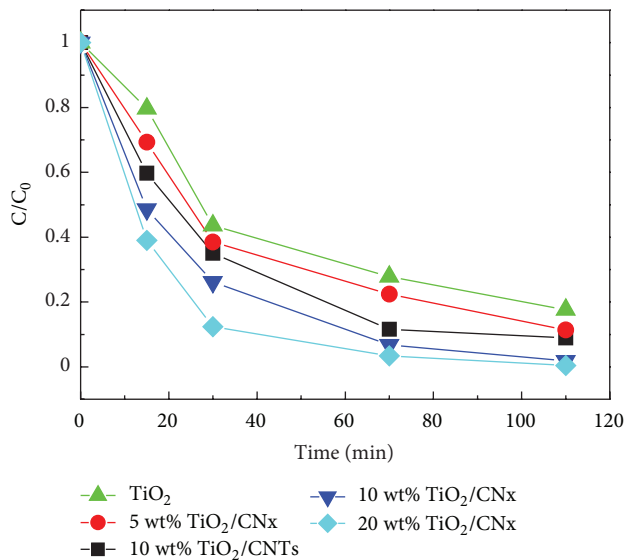
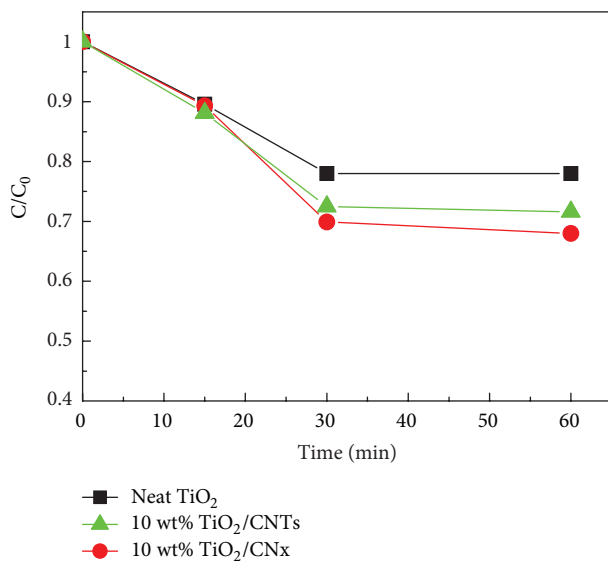FIGURE 5: Comparison of photocatalytic activity between different photocatalysts.



FIGURE 6: Influence of adsorption time on the remaining fraction of MO ($C/C_0$) by neat $TiO_2$, 10 wt% $TiO_2$-CNTs composites, and 10 wt% $TiO_2$-CNx composites.
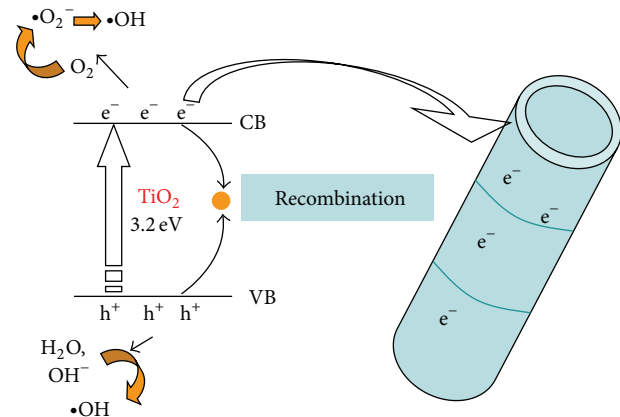


FIGURE 7: Schematic diagram showing band configuration and electron-hole separation at interface of $TiO_2$-CNx nanocomposites under UV irradiation (CB: the bottom of conduction band, VB: the top of valence band).

ratios. Control experiments showed that UV irradiation with no catalyst and catalyst (composite or bare CNx) without irradiation could not degrade MO dye solutions. When $TiO_2$ photocatalyst is used, the degradation efficiency is calculated to be 82.4% at 110 min. When CNTs is introduced, the degradation efficiency is increased to 91.1% for 10 wt% $TiO_2$-CNTs composites and reaches the maximum value of 99.6% for 20 wt% $TiO_2$-CNx composites at 110 min. It is noteworthy that $TiO_2$-CNx composites show superior activity to $TiO_2$-CNTs composites with the same $TiO_2$ weight ratio. With the reaction time at 110 min, the MO degradation efficiency of 10 wt% $TiO_2$-CNTs catalysts is about 91.1%. However, the

value of 10 wt% $TiO_2$-CNx is 98.2%. Hence, $TiO_2$-CNx is an excellent photocatalyst in our experiment.

It has been reported that high adsorption capacities of photocatalysts can lead to the rapid diffusion of MO molecules from solution to the surface of photocatalysts and thus improve photocatalytic performances [20]. Figure 6 shows the remaining fraction of MO ($C/C_0$) in solution during adsorption for 60 min in dark by neat $TiO_2$, $TiO_2$-CNTs composites and $TiO_2$-CNx composites. It is obvious that three photocatalysts exhibited adsorption capacities for MO molecules in the following order: 10 wt% $TiO_2$-CNx > 10 wt% $TiO_2$-CNTs > $TiO_2$. The improved adsorption capacity of 10 wt% $TiO_2$-CNx is attributed to its larger specific surface area of 150.25 $m^2$/g than these of 10 wt% $TiO_2$-CNTs (128.26 $m^2$/g) and neat $TiO_2$ (85.49 $m^2$/g). It is noteworthy that the concentration of MO molecules shows negligible change after 30 min, indicating the adsorption equilibration. So the adsorption is not the main reason for the improvement of photocatalytic activity in our experiment because the mixture was stirred for 30 min in advance. The enhancement of the photocatalytic performance should be mainly ascribed to the promotion of separation rate of photogenerated electron and hole by the formation of heterostructure, as shown in Figure 7.

Under UV irradiation, the valence band electrons of $TiO_2$ can be excited to its conduction bands, giving rise to high-energy electron-hole pairs. Compared with CNTs, CNx has a high degree of defects introduced by nitrogen doping [21]. When the electrons generated by $TiO_2$ transfer into CNx, it could be used as a larger capacity container of electron in comparison with the usual CNTs. So the separation efficiency of electron-hole pairs improved, leading to the dramatically enhanced photoactivity. Moreover, compared to carbon, nitrogen has an extra electron, and from an electronic point of view it is natural to expect an excess of donors in the N-rich areas of the CNTs upon doping [22, 23]. That is to say, impurities significantly enhanced the CNx metallic/conductive character [24]. Hence, the rapid transferring of

electron enhanced separation rate of photogenerated electron and hole.

In order to further explore the effect of the interphase linkage, a mechanical mixture of CNx and $TiO_2$ was prepared. The composition of the mixture was prepared with the same ratio as that in 10 wt% $TiO_2$-CNx nanocomposites. The photocatalytic activity of the mixture photocatalyst was 76.4% at 110 min, much lower than that of 10 wt% $TiO_2$-CNx nanocomposites (98.2%). The low activity is ascribed to CNx in the photocatalyst not being effective in trapping electrons. This lack of effectiveness prevents a decrease in recombination rate. In the mechanical mixture, it is possible that the mechanical mixture process cannot form a strong interphase between the $TiO_2$ and the CNx. In contrast, a strong interphase was formed in $TiO_2$-CNx composites, as evidenced by the previous analysis. Therefore, $TiO_2$-CNx composites showed high activity. Moreover, CNx was almost inactive during MO degradation by UV light irradiation. Once CNx became incapable of bonding strongly with $TiO_2$, they simply occupied the active sites and scattered the incident light. Therefore, the hydrothermal synthesis procedure is a critical factor in forming high-activity $TiO_2$-CNx nanocomposites photocatalysts.

## 4. Conclusions

In this work, we have synthesized uniformly dispersed $TiO_2$ on the surface of CNx via a hydrothermal synthesis method. The nanocomposites showed excellent photocatalytic activity compared with neat $TiO_2$ and $TiO_2$-CNTs. The rapid transferring of electron and high separation efficiency of electron-hole pairs lead to the dramatically enhanced photocatalytic activity. According to the activity and characterization results, the interphase linkage of $TiO_2$ and CNx is a critical factor for promoting photocatalysis. A mechanical mixture cannot provide strong binding between $TiO_2$ and CNx, thus showing decreased activity.

### Acknowledgments

### References

[1] Y. Wang and C. Hong, "$TiO_2$-mediated photomineralization of 2-chlorobiphenyl: the role of $O_2$," *Water Research*, vol. 34, no. 10, pp. 2791–2797, 2000.

[2] K. Tanaka, K. Padermpole, and T. Hisanaga, "Photocatalytic degradation of commercial azo dyes," *Water Research*, vol. 34, no. 1, pp. 327–333, 2000.

[3] A. Fujishima, T. N. Rao, and D. A. Tryk, "Titanium dioxide photocatalysis," *Journal of Photochemistry and Photobiology C*, vol. 1, no. 1, pp. 1–21, 2000.

[4] Q. Xiang, J. Yu, W. Wang, and M. Jaroniec, "Nitrogen self-doped nanosized $TiO_2$ sheets with exposed 001 facets for enhanced visible-light photocatalytic activity," *Chemical Communications*, vol. 47, no. 24, pp. 6906–6908, 2011.

[5] C. Minero and D. Vione, "A quantitative evalution of the photocatalytic performance of $TiO_2$ slurries," *Applied Catalysis B*, vol. 67, no. 3-4, pp. 257–269, 2006.

[6] S. Wang, L. Ji, B. Wu, Q. Gong, Y. Zhu, and J. Liang, "Influence of surface treatment on preparing nanosized $TiO_2$ supported on carbon nanotubes," *Applied Surface Science*, vol. 255, no. 5, pp. 3263–3266, 2008.

[7] W. Wang, P. Serp, P. Kalck, and J. L. Faria, "Photocatalytic degradation of phenol on MWNT and titania composite catalysts prepared by a modified sol-gel method," *Applied Catalysis B*, vol. 56, no. 4, pp. 305–312, 2005.

[8] H. Yu, X. Quan, S. Chen, H. Zhao, and Y. Zhang, "$TiO_2$-carbon nanotube heterojunction arrays with a controllable thickness of $TiO_2$ layer and their first application in photocatalysis," *Journal of Photochemistry and Photobiology A*, vol. 200, no. 2-3, pp. 301–306, 2008.

[9] H. Yu, X. Quan, S. Chen, and H. Zhao, "$TiO_2$-multiwalled carbon nanotube heterojunction arrays and their charge separation capability," *Journal of Physical Chemistry C*, vol. 111, no. 35, pp. 12987–12991, 2007.

[10] S. Aryal, C. K. Kim, K. Kim, M. S. Khil, and H. Y. Kim, "Multi-walled carbon nanotubes/$TiO_2$ composite nanofiber by electrospinning," *Materials Science and Engineering C*, vol. 28, no. 1, pp. 75–79, 2008.

[11] Y. Yao, G. Li, S. Ciston, R. M. Lueptow, and K. A. Gray, "Photoreactive $TiO_2$/carbon nanotube composites: synthesis and reactivity," *Environmental Science and Technology*, vol. 42, no. 13, pp. 4952–4957, 2008.

[12] O. Akhavan, M. Abdolahad, Y. Abdi, and S. Mohajerzadeh, "Synthesis of titania/carbon nanotube heterojunction arrays for photoinactivation of *E. coli* in visible light irradiation," *Carbon*, vol. 47, no. 14, pp. 3280–3287, 2009.

[13] G. Jiang, Z. Lin, L. Zhu, Y. Ding, and H. Tang, "Preparation and photoelectrocatalytic properties of titania/carbon nanotube composite films," *Carbon*, vol. 48, no. 12, pp. 3369–3375, 2010.

[14] A. Jitianu, T. Cacciaguerra, R. Benoit, S. Delpeux, F. Béguin, and S. Bonnamy, "Synthesis and characterization of carbon nanotubes-$TiO_2$ nanocomposites," *Carbon*, vol. 42, no. 5-6, pp. 1147–1151, 2004.

[15] J. Yu, T. Ma, and S. Liu, "Enhanced photocatalytic activity of mesoporous $TiO_2$ aggregates by embedding carbon nanotubes as electron-transfer channel," *Physical Chemistry Chemical Physics*, vol. 13, no. 8, pp. 3491–3501, 2011.

[16] Y. Cong, X. Li, Y. Qin et al., "Carbon-doped $TiO_2$ coating on multiwalled carbon nanotubes with higher visible light photocatalytic activity," *Applied Catalysis B*, vol. 107, no. 1-2, pp. 128–134, 2011.

[17] K. Ghosh, M. Kumar, H. Wang, T. Maruyama, and Y. Ando, "Nitrogen-mediated wet-chemical formation of carbon nitride/ZnO heterojunctions for enhanced field emission," *Langmuir*, vol. 26, no. 8, pp. 5527–5533, 2010.

[18] R. Zhang, L. Li, L. Chen, G. Zhang, and K. Shi, "N-doped carbon nanotubes synthesized in high yield and decorated with $CeO_2$ and $SnO_2$ nanoparticles," *Journal of Alloys and Compounds*, vol. 509, no. 35, pp. 8620–8624, 2011.

[19] L. Wang, L. Wang, H. Jin, and N. Bing, "Nitrogen-doped carbon nanotubes with variable basicity: preparation and catalytic properties," *Catalysis Communications*, vol. 15, no. 1, pp. 78–81, 2011.

[20] R. Leary and A. Westwood, "Carbonaceous nanomaterials for the enhancement of $TiO_2$ photocatalysis," *Carbon*, vol. 49, no. 3, pp. 741–772, 2011.

[21] Y. T. Lee, N. S. Kim, S. Y. Bae et al., "Growth of vertically aligned nitrogen-doped carbon nanotubes: control of the nitrogen content over the temperature range 900–1100°C," *Journal of Physical Chemistry B*, vol. 107, no. 47, pp. 12958–12963, 2003.

[22] S. K. Hong and S. Jeong, "Nitrogen doping and chirality of carbon nanotubes," *Physical Review B*, vol. 70, no. 23, Article ID 233411, 4 pages, 2004.

[23] A. H. Nevidomskyy, G. Csányi, and M. C. Payne, "Chemically active substitutional nitrogen impurity in carbon nanotubes," *Physical Review Letters*, vol. 91, no. 10, Article ID 105502, 4 pages, 2003.

[24] M. Terrones, P. M. Ajayan, F. Banhart et al., "N-doping and coalescence of carbon nanotubes: synthesis and electronic properties," *Applied Physics A*, vol. 74, no. 3, pp. 355–361, 2002.